Model Based Predictive Engine Torque Control for Improved Driveability

Murat ÖTKÜR[1] Orhan ATABAY[2], İsmail Murat EREKE[3]

Ford Otosan, 34885 Sancaktepe İstanbul / Türkiye
İTÜ Makina Fakültesi, 34437 Gümüşsuyu İstanbul / Türkiye
İTÜ Makina Fakültesi, 34437 Gümüşsuyu İstanbul / Türkiye
(Received : 18.03.2016 ; Accepted: 28.04.2016)

ABSTRACT

An engine brake torque based Model Predictive Control (MPC) algorithm with an additional anti-shuffle control element is developed to manipulate the pedal map oriented brake torque demand signal in an automotive powertrain application. In order to capture the longitudinal vehicle dynamics of a front wheel drive vehicle, a simplified 4 mass powertrain model is generated. Model validation is performed with vehicle tests using a typical tip-in and back-out acceleration pedal signal input manoeuvre. Comparison of simulation results and vehicle tests reveals that simplified model is capable of capturing vehicle acceleration profile with the error states for the specified input signals. MPC scheme based on 2 mass vehicle model is developed in "MATLAB / Simulink" environment to obtain a smooth and responsive acceleration profile without error states like excessive jerks and shuffles. An additional engine to wheel speed difference based proportional controller employed in order to further reduce powertrain oscillations without compromising from system response speed. Simulation results indicate that MPC plus P Controller is capable of obtaining desired acceleration and deceleration profiles achieving improved driveability.

Keywords: Drivability, Driveline Modelling, Model Predictive Control.

ÖZ

Bu çalışmada otomobil aktarma organları tork kontrolünde kullanılmak üzere gaz pedalı haritasına bağlı oluşturulan sinyalin düzenlenmesi için, anti-salınım elemanı içeren tork modelli öngörümlü kontrolcü geliştirilmiştir. Önden çekişli bir aracın doğrusal dinamiğini simule etmek için basitleştirilmiş 4 kütleli bir araç modeli kullanılmıştır. Model doğrulaması araç yol testinde gaz pedalına basma ve gaz pedalından çekme manevraları kullanılarak yapılmıştır. Simulasyon ve araç testlerinin karşılaştırılması sonucunda kullanılan 2 kütleli araç modelinin, hata modlarını da içeren araç hızlanma profilini simule etmek için yeterli olduğu görülmüştür. "MATLAB / Simulink" yazılım ortamında "Model Öngörümlü Kontrolcü" kullanılarak sarsıntı ve yüksek salınım gibi hata modları içermeyen ve düzgün ve performanslı bir ivmelenme profili oluşturulmuştur. Mevcut düşük genlikli salınımlar da motor ve araç hızı farkına bazlı çalışan ek bir doğrusal kontrolcü ile tamamen ortadan kaldırılmıştır. Simulasyon sonuçları, "Model Öngörümlü Kontrolcü" nün doğrusal kontrolcü ile birlikte kullanılmasının hızlanma ve yavaşlama manevraları için iyileştirilmiş sürüş özellikleri sağladığını göstermektedir.

Anahtar kelimeler: Sürüş Özellikleri, Aktarma Organları Modellemesi, Model Öngörümlü Kontrol.

1. INTRODUCTION

New technologies as a result of the research and developments activities in electronics resulted with complex electro-mechanical systems equipped automobiles in order to cope with regulatory requirements and elevated customer expectations. As a result, power and torque capability of the modern engines increased significantly in the last decades. Unlike conventional automobiles where acceleration pedal input is mechanically connected to a fuel/air throttle valve, modern vehicles are equipped with electro-mechanical systems where acceleration throttle pedal input signal is captured by an electronic control unit, processed and finally used to control the produced torque and the parameters for the combustion system. When triggered with a high amount of torque change as a result of acceleration pedal response, low frequency oscillations may occur if the driveability calibration of the powertrain is inadequate (Figure 1). These low frequency oscillations correspond to the first resonance frequency of the driveline and typical resonance frequencies are 2-8 Hz depending on gear for manual transmission passenger vehicles [1]. They also interact with human body frequencies and have great impact on driving comfort, therefore need to be avoided.

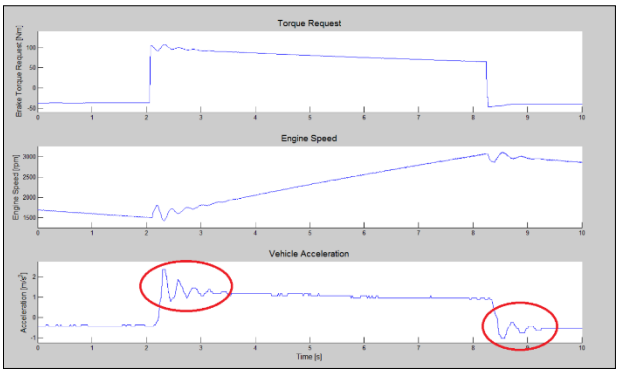

Fig. 1. Vehicle response for a tip-in & tip-out response showing error states; Top sub-figure: Engine brake torque request, Mid sub-figure: Engine speed measurement, Bottom sub-figure: Vehicle longitudinal acceleration measurement.

*Sorumlu Yazar (Corresponding Author)
e-posta: motkur@ford.com
Digital Object Identifier (DOI) : 10.2339/2017.20.1 71-82

Automotive manufacturers' engine control algorithms already employ so-called anti-jerk feature. Anti-jerk works in an open loop manner using look-up tables and main control strategy is to slew the pedal oriented torque request especially in backlash transition region and do not have close loop feedback control. The drawback of anti-jerk feature is it is a subjective calibration methodology and outcome is strongly dependant on calibrator's performance. Additionally filling look-up tables for all gear, engine speed and pedal position combinations requires significant amount of development time. Considering these obstacles of the current driveability features, the subject of automated torque control for improved driveability attracts attention of many automotive manufacturers and researches as it can be described as an optimization problem dealing with performance and comfort counter measures.

There are a large number of studies reported in the area of automated engine torque control.

Fredriksson et al. was one of the first researchers that employed the idea of using engine as an actuator in order to actively damp the powertrain oscillations [2]. Subjected study involves different linear controllers such as PID, "Pole Placement" and "LQG/LTR" controllers. These were assessed using criteria like transient performance, parameters and noise sensitivity. The proposed "LQG/LTR" controller is evaluated as the most suitable of the investigated controllers as it is easy to tune, works satisfactory both in simulations as well as in real field trials. Baumann et al. developed two different control methodologies for anti-jerk control: A H_∞ controller using mixed sensitivity approach [3] and a model based predictive controller using Smith predictor approach to cover the system inherent dead-time [4], controller gains were determined using root locus method. Both studies uses speed difference as input variable and produces corrective torque as output. An analogy to classical PD-controller has been drawn and superiority of the proposed methodology is demonstrated on the latter study. Similarly Pettersson and Nielsen proposed a speed-control strategy that included the behaviour of the driveline in the control scheme [5]. The model based state-feedback controller calculates fuel amount reducing the low frequency driveline oscillations. Berriri et al. developed a partial torque compensator in order to actively damp powertrain oscillations [6]. Like the previous studies the controller employs the engine speed as input to provide the corrective torque that will oppose to the shuffle. The study differs from previous studies in that the control synthesis is more or less independent of the driveline characteristics and non linearities using a simplified model of the engine without the precise characteristics of the driveline. Superiority of the methodology is that it may be tuned directly on the vehicle, considering the fact that post design tuning parameters are few and with clear meanings, the benefit over the previous approaches is a reduced cost and time for development. Webersinke et al. proposed two linear quadratic controllers: a comfort controller, which damps the driveline oscillations and a dynamic controller which guarantees a high dynamical performance [7]. Both control algorithms show improvement on system performance: enhanced driving comfort with reduced driveline resonances without loss of dynamics. Templin et al. developed an LQR-formulation of a driveline anti-jerk controller which acts as a torque compensator which does not require any state reference trajectories [8]. The controller is extended with an optimization based handling of the backlash transition that limits the shunt phenomenon [9]. At both of the studies, results were verified by measurements in a heavy duty truck and show good improvement with respect to non-controller case. As a discrepancy to the previous studies He et al. established a torque-based nonlinear predictive control approach with an additional torque load estimation component [10]. Torque load estimation component is based on a mean value model of the internal combustion engine. A proportional-integral observer is employed to estimate the torque load of the powertrain and a torque-based nonlinear predictive controller is designed by use of iterative optimization. One of the latest studies on the subject topic is held by Fang et al. [11]. Subjected study involves a new model reference approach using engine speed as a control objective letting the engine speed output follow the referred speed at any time by forcing the plant transfer function. A comparison of the used methodology with classical state space and PID controllers shows that the proposed controller had better performance on speed, acceleration and torque control aspects.

2. DRIVELINE MODELLING

Vehicle powertrain consists of various components starting from engine to tyres. These are complex structures such as flywheel, clutch, gearbox, differential (final drive), drive shafts and wheels (Figure 2) forming a high order system including nonlinearities even for a front wheel drive (FWD) vehicle. Although most of the components are made from steel, due to high amount of torque transported and geometrical constrains, the overall system cannot be treated as completely rigid.

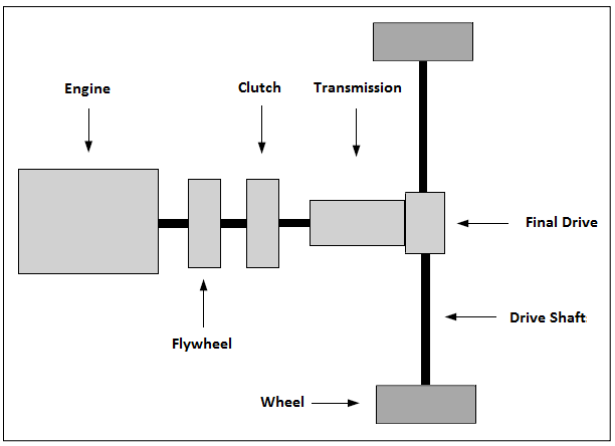

Fig. 2. Components of vehicle driveline for a FWD vehicle.

Especially because of the components with spring mechanisms such as dual mass flywheel (DMF) and clutch, shape of the drive shafts - long cylinders with a small diameter (hollow in some applications); when triggered by a large amount of torque, the response of the overall system degrades compared to a rigid system. In order to utilize a controller mechanism a simplified model that is capable of capturing the system dynamics is required. Several driveline models have been proposed in the literature, 2 mass models are the most common ones. This study composes of 2 different driveline models: a 4 mass vehicle model with road load component for simulating longitudinal vehicle dynamics and a simplified 2 mass vehicle model for controller utilization purpose. It has been verified that 2 mass vehicle model is accurate enough to employ the model based predictive torque control algorithm. As the aim of this study is to develop a close loop driveability algorithm for real world applications, 4 mass vehicle model is used as replacement environment for the subjected vehicle in order to employ 2 mass vehicle model based control algorithm. 4 mass vehicle model validation is performed with vehicle tests and had showed good results.

2.1. Four Mass Vehicle Model

When studying driveline of a front wheel drive vehicle, clutch and drive shafts are subjected to relatively highest torsional deformation resulting possibility for oscillations. In order to capture longitudinal vehicle dynamics characteristics these components should be modelled with flexible elements (Figure 3).

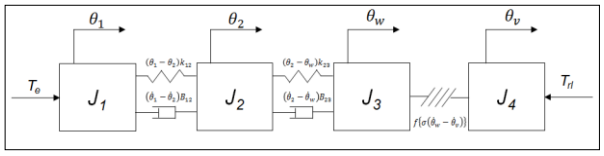

Fig. 3. Free body diagram of 4 mass vehicle model with 4 inertias connected by 2 spring damper elements and tyre.

4 mass vehicle model consists of the components below:

- Integrated inertia node 1 (J_1): Engine, flywheel, clutch primary side
- Flexible element # 1: Clutch
- Integrated inertia node 2 (J_2): Clutch secondary side, transmission, final drive
- Flexible element # 2: Drive shafts
- Wheel and tyre inertia, node 3(J_3)
- Tyre dynamics
- Vehicle inertia, node 4 (J_4)

Applying Newton's second law to each of the inertia components results with below differential equations.

$$J_1 \cdot \ddot{\theta}_1 = T_e - (\theta_1 - \theta_2).k_{12} - (\dot{\theta}_1 - \dot{\theta}_2).B_{12} \quad (1)$$

$$J_2 \cdot \ddot{\theta}_2 = (\theta_1 - \theta_2).k_{12} + (\dot{\theta}_1 - \dot{\theta}_2).B_{12} - (\theta_2 - \theta_w).k_{23} - (\dot{\theta}_2 - \dot{\theta}_w).B_{23} \quad (2)$$

$$J_3 \cdot \ddot{\theta}_w = (\theta_2 - \theta_w).k_{23} + (\dot{\theta}_2 - \dot{\theta}_w).B_{23} - f\{\sigma(\dot{\theta}_w - \dot{\theta}_v)\} \quad (3)$$

$$J_4 \cdot \ddot{\theta}_v = f\{\sigma(\dot{\theta}_w - \dot{\theta}_v)\} - T_{rl} \quad (4)$$

where

- θ_x, $\dot{\theta}_x$and $\ddot{\theta}_x$are the angular position, velocity and acceleration of the x[th] node respectively,
- k_{xy} and B_{xy} are the stiffness and damping coefficients of the spring-damper elements between x[th] and y[th] nodes respectively,
- T_e is the generated engine brake torque at crankshaft level,
- Road load is modelled as the sum of the aerodynamic, rolling and grade resistance forces as below (x),

  $$T_{rl} = r_w.(F_{aero} + F_{rr} + F_g) \quad (5)$$

  where

  - $F_{aero} = \frac{1}{2}.\rho_{air}.C_D.v^2$ (6)
  - $F_{rr} = m_{tot}.g.cos(\alpha).f_r$ (7)
  - $F_g = m_{tot}.g.sin(\alpha)$ (8)
- $f\{\sigma\}$ is the tyre/road friction force function,
- J_1 is the total inertia of engine, flywheel and clutch primary side,

  $$J_1 = J_e + J_{fw} + J_{cp} \quad (9)$$
- J_2 is the total inertia of clutch secondary side, transmission, final drive and drive shafts,

  $$J_2 = J_{cs} + \frac{J_t}{i_t^2} + \frac{J_{fd}}{i_t^2.i_f^2} + \frac{J_{ds}}{i_t^2.i_f^2} \quad (10)$$

  where

  - i_t is the reduction ratio of the selected gear
  - i_f is the reduction ratio of the final gear
- J_3 is the total inertia of wheels including tyres at crankshaft level

  $$J_3 = 4\frac{J_w}{i_t^2.i_f^2} \quad (11)$$
- J_4 is the total inertia of the vehicle mass at crankshaft level

  $$J_4 = m_{tot}.\left(\frac{r_w}{i_t^2.i_f^2}\right)^2 \quad (12)$$

Flexible elements (clutch and driveshafts) in the vehicle model were modelled using spring/damper simulation block generated in "MATLAB / Simulink". This block aims to accurately calculate the torque generated when a displacement occurs on either side.

Tyre dynamics is simulated using the well-known Pacejka's magic tyre formula [12]. Tyre slip is calculated via dividing the speed delta between the tyre circumference and the vehicle with absolute vehicle

speed. The coefficient of friction within the tyre-road interface is obtained from a lookup table and used to calculate the tractive effort.

2.2. Two Mass Vehicle Model for Controller Design

Due to high level of nonlinearities at the 4 mass vehicle model, model predictive control algorithm cannot be operated successfully. Therefore a simplified 2 mass vehicle model with road load component has been developed for the model predictive controller plant usage. Driveshafts have been assumed as the main source for the elasticity, resulting a 2 mass system combined with a spring / damper element (Figure 4).

2-mass vehicle model consists of components below:

- Integrated inertia node 1 (J_1): Engine, flywheel, clutch primary & secondary sides, transmission and final drive
- Flexible element # 1: Driveshafts
- Integrated inertia node 2 (J_2): Wheels, tyres and vehicle

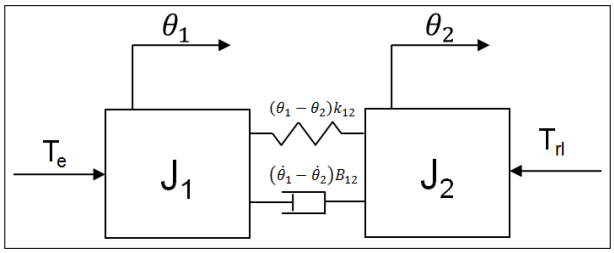

Fig. 4. Free body diagram of simplified 2 mass vehicle model.

Applying Newton's second law to each of the inertia components results with below differential equations.

$$J_1 \cdot \ddot{\theta}_1 = T_e - (\theta_1 - \theta_2).k_{12} - (\dot{\theta}_1 - \dot{\theta}_2).B_{12} \quad (13)$$

$$J_2 \cdot \ddot{\theta}_2 = (\theta_1 - \theta_2).k_{12} + (\dot{\theta}_1 - \dot{\theta}_2).B_{12} \quad (14)$$

where

- θ_x, $\dot{\theta}_x$and $\ddot{\theta}_x$are the angular position, velocity and acceleration of the x[th] node respectively,
- k_{12} and B_{12} are the stiffness and damping coefficients of modelled the spring-damper elements of the drive shafts respectively,
- T_e and T_{rl} are engine brake torque and road load resistive torque calculated at crankshaft level respectively,
- J_1 is the total inertia of engine, flywheel, clutch primary & secondary sides, transmission, final drive

$$J_1 = J_e + J_{fw} + J_{cp} + J_{cs} + \frac{J_t}{i_t^2} + \frac{J_{fd}}{i_t^2.i_f^2} \quad (15)$$

- J_2 is the total inertia of drive shafts, wheels, tyres and vehicle mass

$$J_2 = \frac{J_{ds}}{i_t^2.i_f^2} + 4.\frac{J_w}{i_t^2.i_f^2} + m_{tot}.\left(\frac{r_w}{i_t^2.i_f^2}\right)^2 \quad (16)$$

3. VALIDATION OF SIMULATION RESULTS VIA VEHICLE TESTS

4 mass vehicle model validation was performed via real world experiments carried out on a CD class front wheel drive (FWD) passenger vehicle equipped with a diesel engine. The engine had a regulated 2 stage (R2S) turbocharger system. Vehicle had a 6 speed wet dual clutch transmission and test weight was approximately 2125 kg. Engine and vehicle properties are summarized in Table 1. Tests were performed at manual mode and transmission kick-down function – which downshifts automatically if the accelerator brake pedal is pressed more than a certain position (close to maximum) very rapidly - had been disable in order to reach maximum torque without downshifting during the wide open throttle (WOT) manoeuvre. Gearbox had torque truncation protection in low gears; therefore test manoeuvres were done at 3rd and 4th gears where maximum allowed torque values are 400 Nm and 450 Nm respectively. Test manoeuvre consists of a stabilized deceleration with zero accelerator pedal position from 2400 rpm to 2000 rpm engine speed followed by sudden tip-in to 100% pedal position with engine speed acceleration up to 3000 rpm. Manoeuvre is finalized a quick tip-out of the accelerator pedal to 0% and stabilized deceleration to 2500 rpm engine speed Figure 5). All ECU driveability features like anti-jerk and anti-shuffle were disabled in order to get an unfiltered torque request from the pedal input. Black smoke limitation feature was not turned off as disabling the feature will provide torque error such that injected fuel will not burn completely due to lack of combustion air, resulting degradation on vehicle model validations. Engine speed, vehicle speed, vehicle acceleration and ECU estimated brake torque signals were captured online via direct A7 connection to ECU.

Table 1. Engine and vehicle properties.

Engine Displacement	2.0 lt
Number of Cylinder	4
Rated Power	210PS (3750
Rated Torque	450 Nm (2000-
Transmission	6 Speed
Drive Wheel Configuration	Front Wheel
Final Drive Ratio	3.55
Tire Dimensions	245/50R17
Test Weight	2125 kg

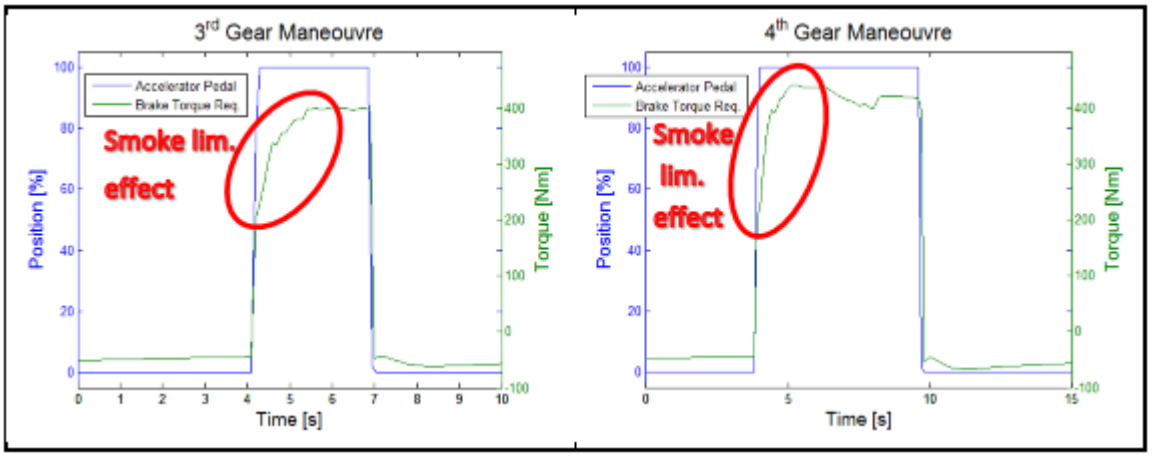

Fig. 5. Accelerator pedal position and brake torque request trace for the 3rd and 4th gear tip-in and tip-out manoeuvres.

Comparison of simulation results with vehicle measurements shows that 4 mass vehicle model is capable of simulating vehicle characteristics. Figure 6 contains vehicle acceleration, vehicle speed and engine speed response for a 3rd gear tip-in and tip-out manoeuvre. Acceleration axis has been normalized in terms of securing intellectual properties. Comparison of simulation and vehicle measurements clearly identifies that 4 mass vehicle model reflects subjected quantities in good correlation with vehicle measurements. For steady state conditions (stabilized deceleration and acceleration) proposed model delivers precise predictions, ensuring good accuracy of engine and vehicle parameters used in the model. Zoomed view of vehicle longitudinal acceleration comparison ensures that proposed vehicle model successfully captures powertrain characterization as amplitude and frequency of the oscillation are in good alignment (Figure 7). However damping rate of the oscillations is slightly lower at the simulations. This is mainly due to pitch motion of the vehicle. Vehicle longitudinal acceleration sensor is mounted to the chassis and proposed vehicle model do not contain any powertrain – chassis connection mechanisms such as suspension system and assumed completely rigid. Therefore pitch motion is not captured at the proposed vehicle model. Figures 8 and 9 contains vehicle acceleration, vehicle speed and engine speed response for 4th gear tip-in and tip-out manoeuvres. Comparison of simulation and vehicle measurements shows that simulation results are in good alignment with the vehicle measurements for 4th gear tip-in and tip-out manoeuvres.

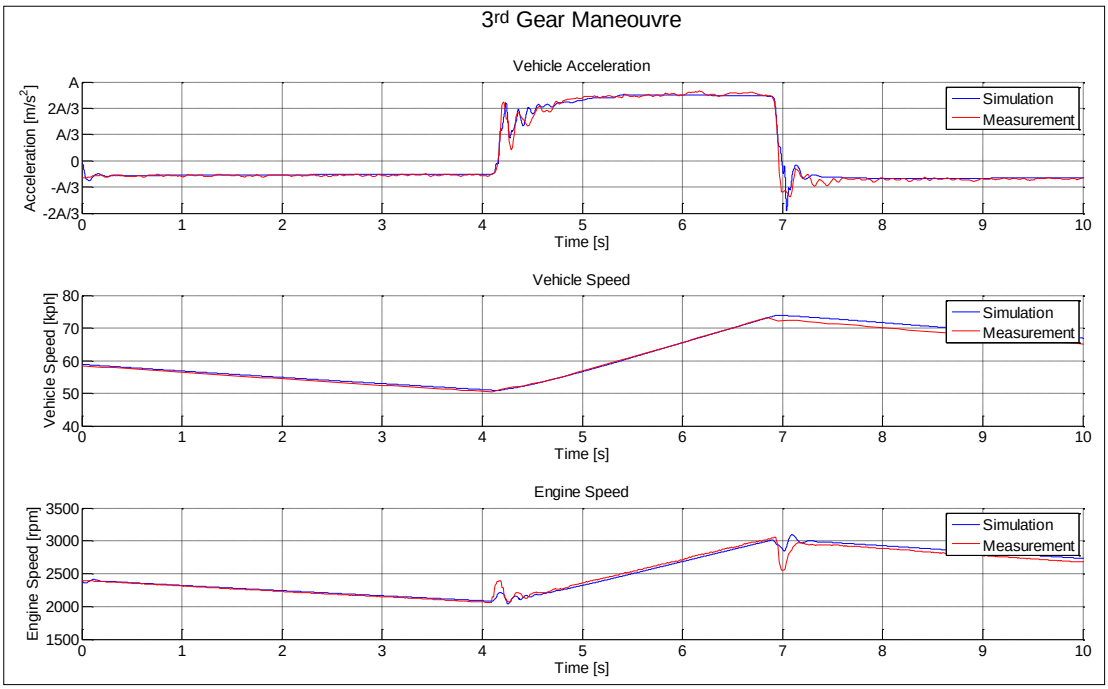

Fig. 6. Comparison of vehicle measurements and simulation results for 3rd gear tip-in and tip-out manoeuvre; Top sub-figure: Vehicle longitudinal acceleration, Mid sub-figure: Vehicle speed, Bottom sub-figure: Engine

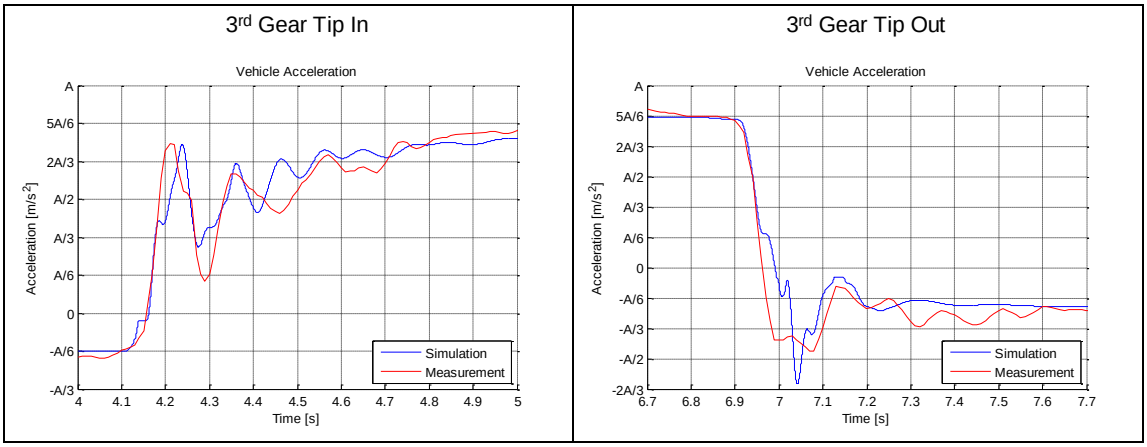

Fig. 7. Comparison of vehicle longitudinal acceleration measurement and simulation results for 3rd gear tip-in (left) and tip-out manoeuvres (right).

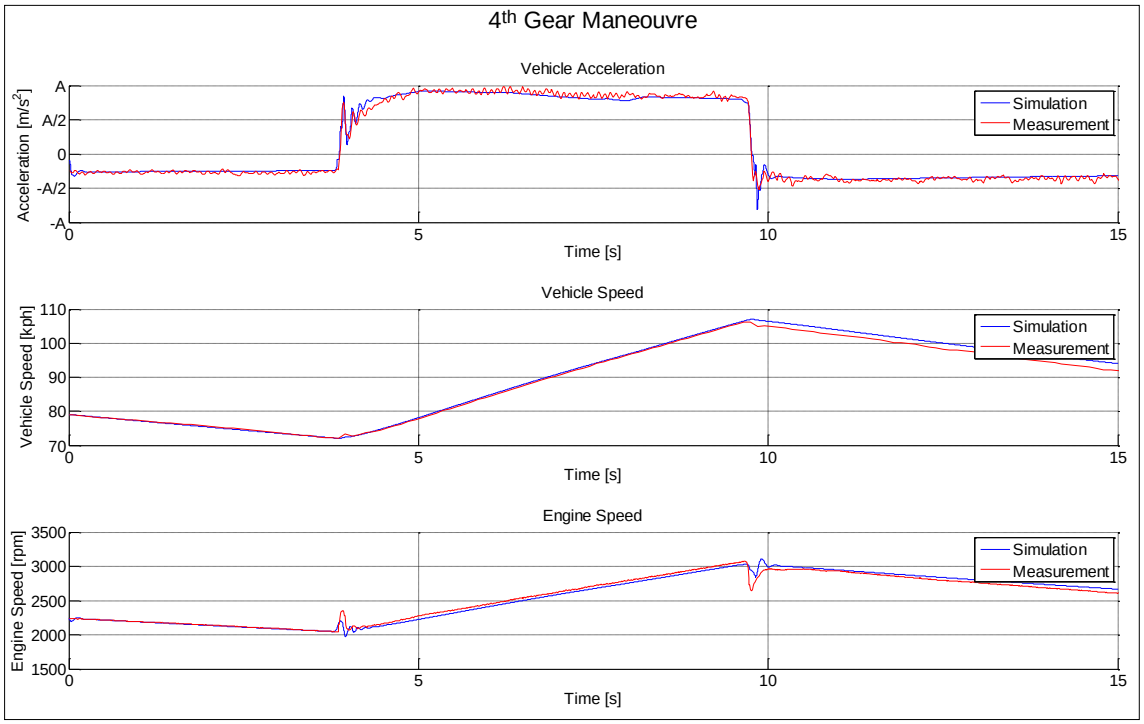

Fig. 8. Comparison of vehicle measurements and simulation results for 4th gear tip-in and tip-out manoeuvre; Top sub-figure: Vehicle longitudinal acceleration, Mid sub-figure: Vehicle speed, Bottom sub-figure: Engine speed.

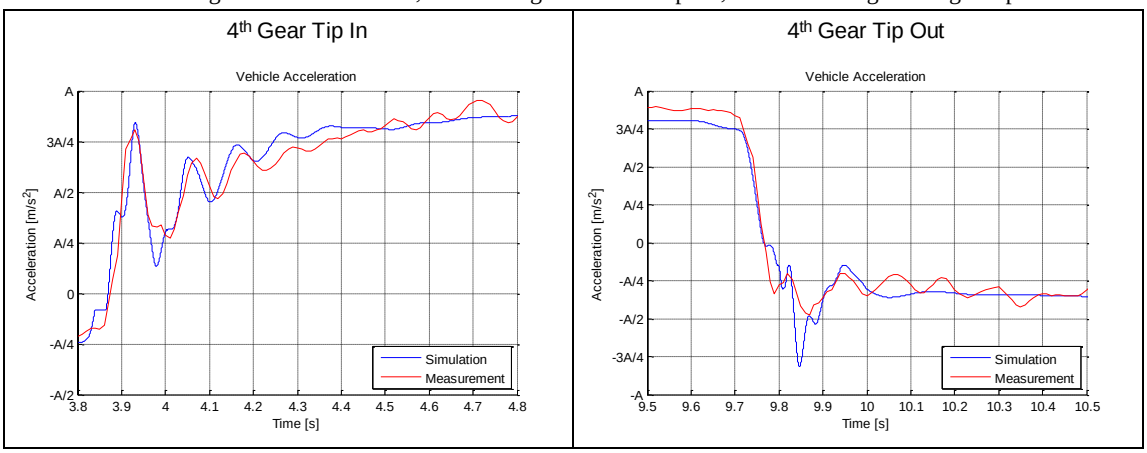

Fig. 9. Comparison of vehicle acceleration measurement and simulation results for 4th gear tip-in (left) and tip-out manoeuvres (right).

4. CONTROLLER DESIGN

MPC can be used for longitudinal vehicle torque control due to its ability to handle input and output constraints under finite horizon constrained optimal control framework. Once plant model is defined accurately, tuning of the MPC is easy due to intuitive controller concept. Moreover MPC includes feed forward control that acts against measured disturbances such as accessory losses in automotive applications which favours usage in automotive torque control applications, however accessory losses are not subjected within the content of this study.

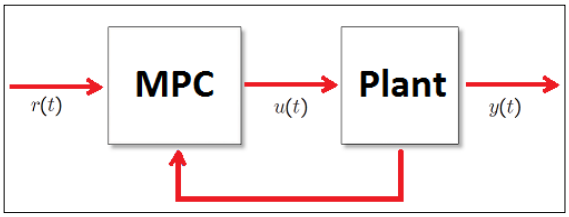

Fig. 10. Model based predictive control concept.

A basic formulation of the cost function used at the optimizer of the MPC can be described as follows:

$$\min_{u_t,\dots,u_{t+N-1}} \{\sum_{k=0}^{N-1} \|y_{t+k} - r(t)\|^2 + \rho\|u_{t+k} - u_r(t)\|^2\} \quad (17)$$

subjected to

$$\begin{aligned} x_{t+k+1} &= f(x_{t+k}, u_{t+k}) \\ y_{t+k} &= g(x_{t+k}, u_{t+k}) \\ u_{min} &\le u_{t+k} \le u_{max} \\ y_{min} &\le y_{t+k} \le y_{max} \\ x_t &= x(t), k = 0, \dots, N-1 \end{aligned} \quad (18)$$

Where u_{min} and u_{max} are the plant input constrains, for the subjected problem friction torque and maximum available torque, similarly y_{min} and y_{max} are the minimum and maximum acceleration quantities for that specific gear. Constraining inputs is definitely required due to the fact that MPC controller can result with a higher torque request that the engine can deliver.

For the proposed study MPC setup parameters are defined as follows (Figure 11):

- Control interval: 0.01s
- Predicted horizon intervals: 100
- Control horizon intervals: 40

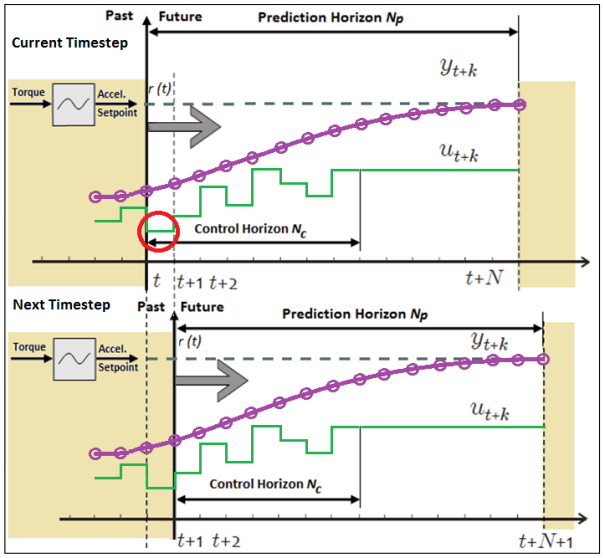

Fig. 11. MPC operation for single input single output system.

MATLAB/Simulink model of the 2 mass vehicle model with controller is shown at figure 12. Road load resistant force at crankshaft level is subtracted from the driver acceleration pedal request torque and multiplied by 1/total inertia value in order to achieve the vehicle acceleration request which is used as the reference desired setpoint value for the MPC controller. Modelled vehicle acceleration value is taken as the input to the controller with engine brake torque values as the control variable. Additional P controller using engine and vehicle speed difference value as input variable generates a

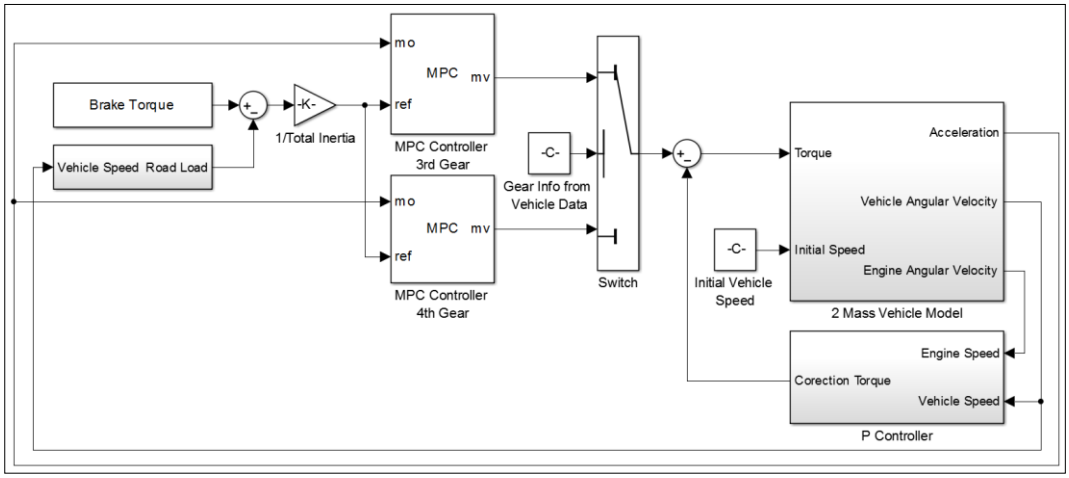

Fig. 12. MATLAB/Simulink model with MPC & P-controller.

corrective torque which is subtracted from the MPC controller output value in order to obtain a smoother acceleration profile.

MATLAB/Simulink model of the 2 mass vehicle model is shown at figure 13. 2 inertias (Figures 14 & 15) were combined with spring damper element (Figure 16). Nonlinear spring and damper characteristics of the driveshafts were embedded in look up tables. Although the stiffness output is a function of torsion generated on the component, the damping torque is set to zero when the stiffness torque is zero. This has been implemented to model the backlash, where the damping forces disappear.

5. COMPARISON OF CONTROLLER PERFORMANCE

As shown at the previous sections applying pedal map based torque request without any driveability corrections results with high amplitude initial kick followed by fading oscillations for tip-in and tip-out manoeuvres. A 2 mass vehicle model based MPC controller had been utilized in order to actively control the engine brake torque in order to have a smooth vehicle acceleration response without shuffles and compromising from response speed. Modifying weight tuning factor in MPC setting defines system response speed. Increasing weight

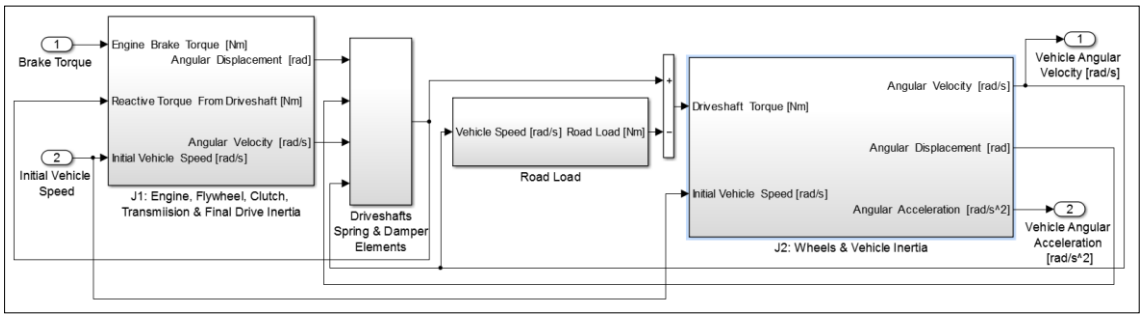

Fig. 13. MATLAB/Simulink 2 mass vehicle model.

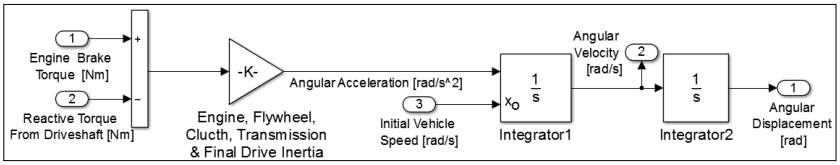

Fig. 14. MATLAB/Simulink J1 inertia block.

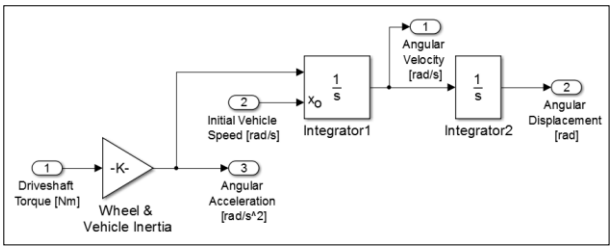

Fig. 15. MATLAB/Simulink J2 inertia block.

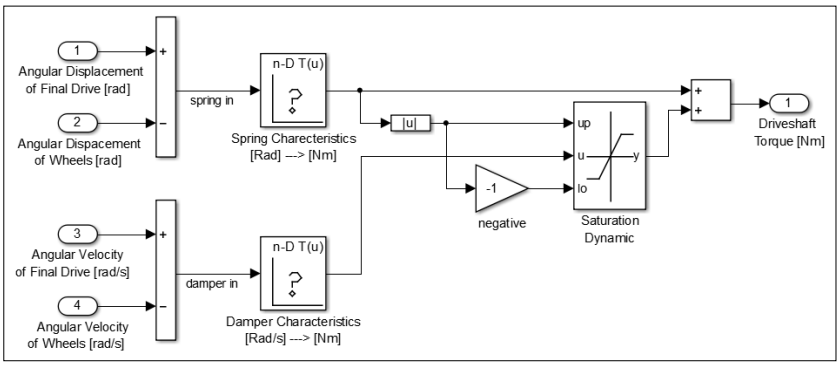

Fig. 16. MATLAB/Simulink driveshafts spring & damper simulation block.

rate results with faster response with a compromise from system robustness forming low frequency oscillations. Introduction of the additional P controller based on engine and vehicle speed difference, assists to further reduce the remaining oscillations without renouncing from system response speed. 3rd gear tip-in and tip-out manoeuvres results are showed at figure 17. Engine and vehicle speed profiles are very similar for the proposed controllers. Zoomed acceleration graphs in figure 18 clearly show that when compared to no controller case both MPC and MPC + P controllers provide smoother vehicle acceleration and deceleration response which will definitely improve comfort characteristics of the vehicle. Additionally system response rate degradation with respect to no controller case is very small. For both controllers initial response delay is lower than 0.04 seconds. Rise time delay of MPC and MPC + P controllers with respect to no controller case is 0.1 seconds for the tip-in manoeuvre. Similarly rise time delay of MPC and MPC + P controllers with respect to no controller case is 0.1 and 0.2 seconds respectively for the tip-out manoeuvre. Figure 19 shows the torque request from the engine. For both controllers torque rise rate is slightly lower than the no controller case and additional P controller results with %10 less torque request up to 0.5 seconds from the beginning of tip-in and tip-out manoeuvres.

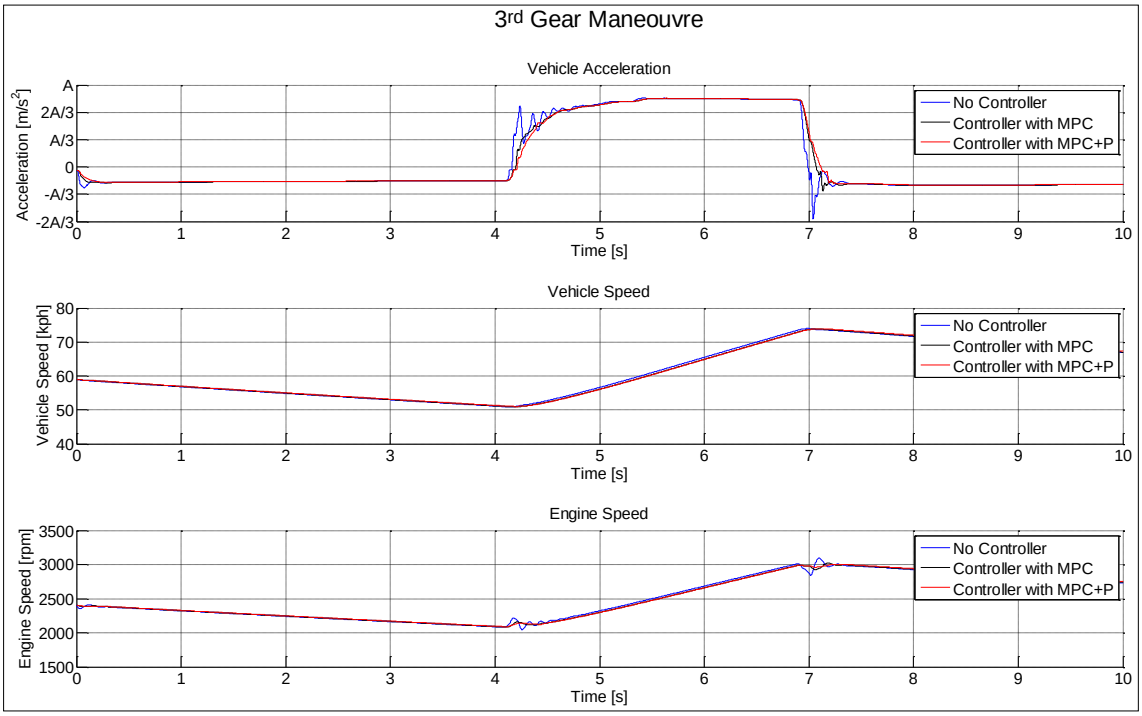

Fig. 17. Comparison of simulation results of no-controller, MPC & MPC + P controller for 3rd gear tip-in and tip-out manoeuvre; Top sub-figure: Vehicle longitudinal acceleration measurement, Mid sub-figure: Vehicle speed, Bottom sub-figure: Engine speed.

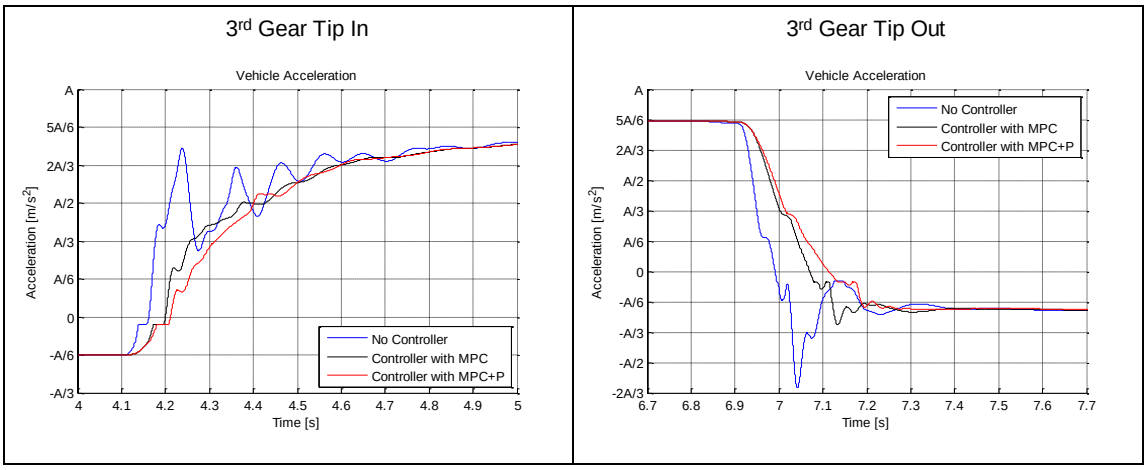

Fig. 18. Comparison of simulation results of no-controller, MPC & MPC + P controller for 3rd gear tip-in (left) and tip-out manoeuvres (right).

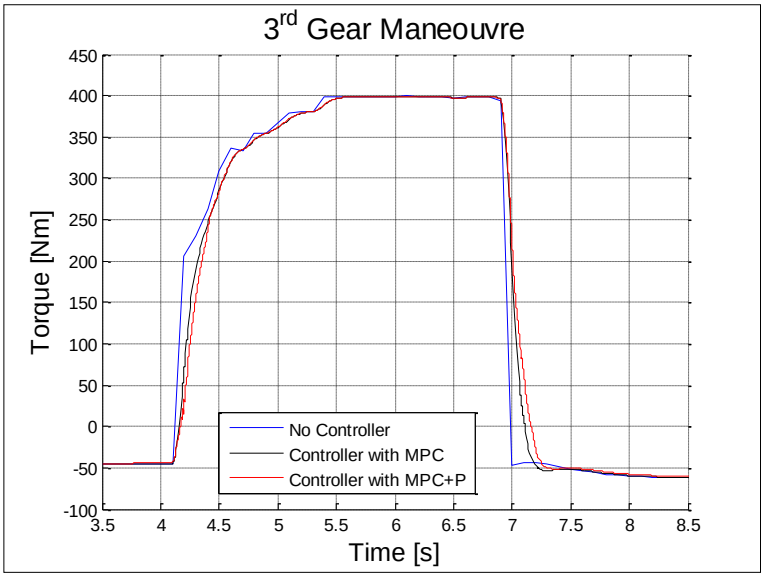

Fig. 19. Comparison of engine torque for simulation results of no-controller, MPC & MPC + P controller for 3rd gear tip-in and tip-out manoeuvre.

4th gear tip-in and tip-out manoeuvres' results are shown at figure 20. Engine and vehicle speed profiles are very similar for the proposed controllers as in the case with 3rd gear manoeuvres. For both controllers initial response delay is lower than 0.04 seconds (Figure 21). Rise time delay of MPC and MPC + P controllers with respect to no controller case is 0.1 seconds for the tip-in manoeuvre. Similarly rise time delay of MPC and MPC + P controllers with respect to no controller case is 0.15 and 0.2 seconds respectively for the tip-out manoeuvre. Figure 22 shows the torque request from the engine. For both controllers torque rise rate is slightly lower than the no controller case and additional P controller results with %10 less torque results up to 0.3 seconds from the beginning of tip-in and tip-out manoeuvres.

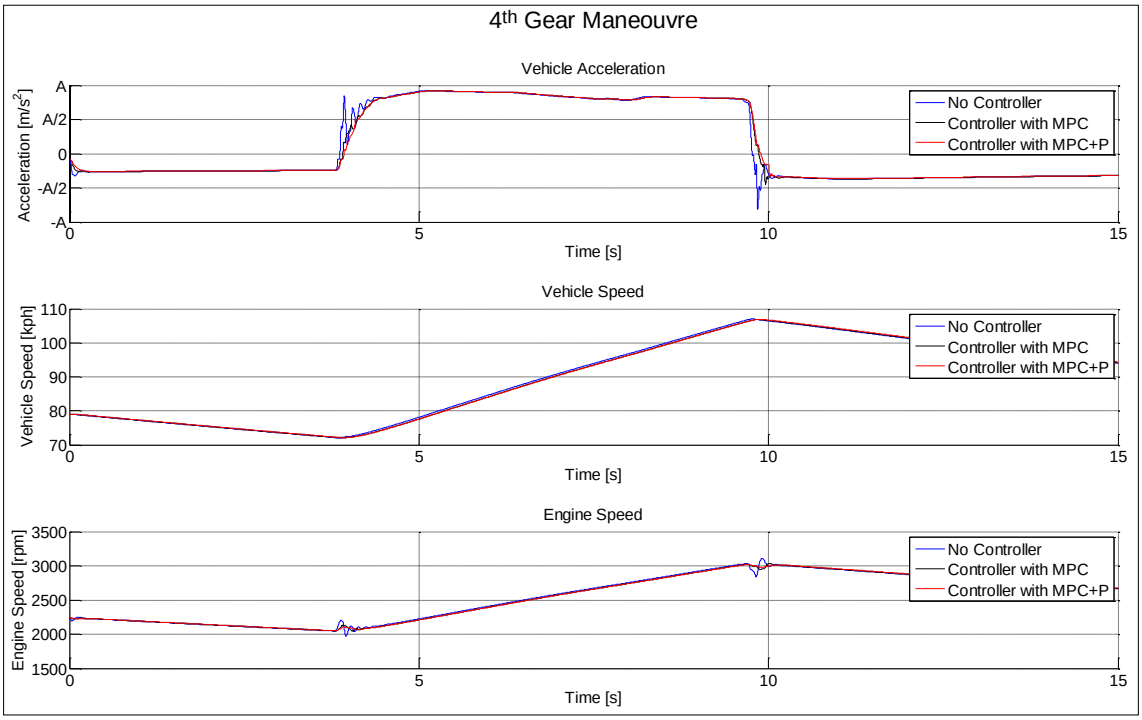

Fig. 20. Comparison of simulation results of no-controller, MPC & MPC + P controller for 4th gear tip-in and tip-out manoeuvre; Top sub-figure: Vehicle longitudinal acceleration measurement, Mid sub-figure: Vehicle speed, Bottom sub-figure: Engine speed.

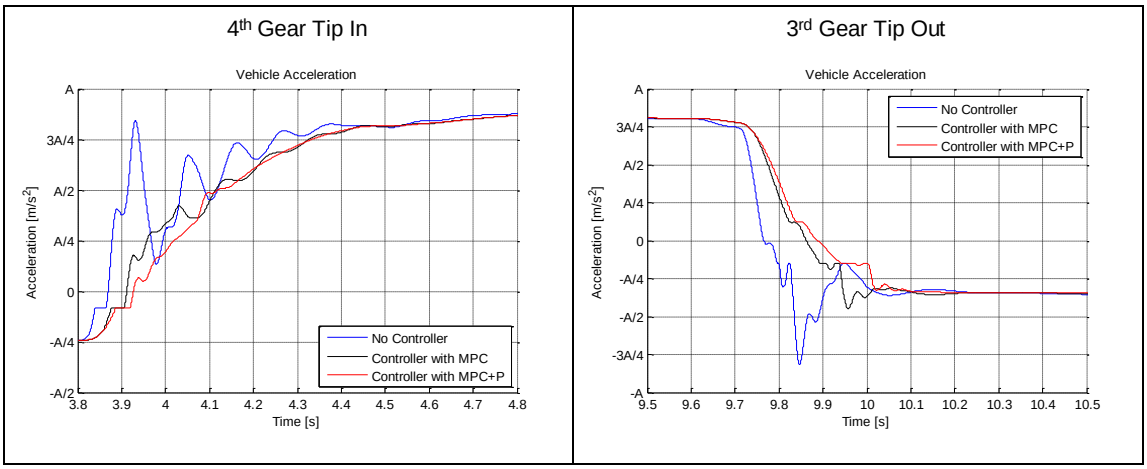

Fig. 21. Comparison of simulation results of no-controller, MPC & MPC + P controller for 4th gear tip-in (left) and tip-out manoeuvres (right).

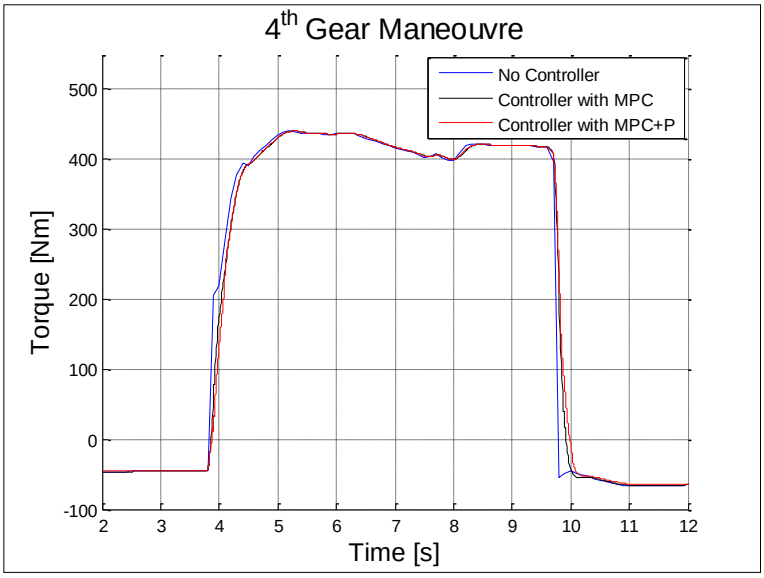

Fig. 22. Comparison of engine torque for simulation results of no-controller, MPC & MPC + P controller for 4th gear tip-in and tip-out manoeuvre.

6. CONCLUSION

This paper describes a torque based MPC algorithm design which contains the behaviour of the driveline with 2 DOF system in the control scheme, to attenuate the powertrain oscillations in longitudinal vehicle motion control. An additional anti-shuffle control element, basically a P controller based on the speed difference of engine and vehicle speeds, has been implemented to the MPC control algorithm to improve the powertrain oscillations without compromising from overall system response speed. It has been demonstrated that employing MPC controller is very effective once the plant of the system has been identified. Weight tuning functionality of the MPC controller provides users the ability to determine system response with robustness and faster system response counter measures. Moreover an additional P control element enables a faster and more smooth/stable response. With the proposed methodology, a calibration engineer will only be required to determine the MPC controller weight tuning coefficient and P controller gain which results with an easy to calibrate methodology for longitudinal vehicle control.

FUTURE WORK

Proposed algorithm bases on the fact that requested torque will be generated from the internal combustion engine. However in turbocharged diesel engines due to boost lag phenomenon, a difference between requested and produced torque is present. With modern engine air path control algorithms, boost response of the turbocharged engine significantly improved, on the other hand due to elevated torque levels torque reporting deviation is inevitable. Within this scope an engine brake torque estimation model has been developed [13]. Future work of this study will be combining engine brake torque estimation model with the longitudinal vehicle control algorithm.

SYMBOLS

J : Moment of inertia [kgm^2]
T : Torque [Nm]
k : Torsional spring coefficient [Nm/rad]
B : Torsional damper coefficient [Nm.s/rad]
C_D : Drag coefficient [-]
F : Force [Nm]
f_r : Rolling coefficient [-]
r : Radius [m]
g : Gravity [m/s^2]
i : Gear ratio [-]
m : Mass [kg]
v : Velocity [m/s^2]

INDICES

1 : Equivalent node for engine, flywheel, clutch primary side (4 mass model) Equivalent node for engine, flywheel, clutch primary & secondary sides, final drive (2 mass model)
2 : Equivalent node for clutch secondary side, transmission, final drive (4 Mass Model) Equivalent node for wheels, tyres and vehicle (2 mass model)
3 : Equivalent node for wheels and tyres
4 : Equivalent node for vehicle
e : Engine
rl : Road Load
air : Air
aero: Aerodynamic
rr : Rolling resistance
g : Gravitational
fw : Flywheel
cp : Clutch primary side
cs : Clutch secondary side
t : Reduction ratio of the selected gear
f : Reduction ratio of the final gear
w : Wheel
v : Vehicle
tot : All driveline components and vehicle

GREEK LETTERS

θ : Angular position [rad]
$\dot{\theta}$: Angular velocity [rad/s]
$\ddot{\theta}$: Angular acceleration [rad/s^2]
ρ : Density [kg/m^3]
α : Road gradient [rad]
σ : Pacejkatyre model coefficient [Nm/% slip]

REFERENCES

1. De La Salle S., Jansz M. and Light D., "Design of feedback control system for damping of vehicle shuffle", ***EAEC conference***, Barcelona, 1-10, (1999).
2. Fredriksson J., Weifors H., and Egardt B., "Powertrain control for active damping of driveline oscillations", ***International Journal of Vehicle System Dynamics***, 37(5): 359-376, (2002).
3. Baumann J., Swarnakar A. and Kiencke U., "A robust controller design for anti-jerking", ***SAE Technical Paper***, No: 01-0041, (2005).
4. Baumann J., Torkzadeh D., Ramstein A., Kiencke U. and Schlegl, T., "Model-based predictive anti-jerk control", ***Control Engineering Practice***, 14: 259-266, (2006).
5. Pettersson M. and Nielsen L., "Diesel engine speed control with handling of driveline resonances", ***Control Engineering Practice***, 11: 319-328, (2003).
6. Berriri M., Chevrel P., Lefebvre D., and Yagoubi, M., "Active damping of automotive powertrain oscillations by a partial torque compensator", ***American Control Conference***, New York, 5718-5723, (2007).
7. Webersinke L., Augenstein L. and Kienche, U., "Adaptive linear quadratic control for high dynamical and comfortable behaviour of a Heavy Truck", ***SAE Technical Paper***, No: 01-0534, (2008).
8. Templin P. and Egardt, B., "An LQR torque compensator for driveline oscillation damping", ***IEEE International Conference on Control Applications***, Saint Petersburg, 352-356, (2009).
9. Templin, P. and Egardt, B., "A powertrain LQT-torque compensator with backlash handling", ***Oil & Gas Science and Technology – Rev. IFP Energies nouvelles***, 66(4): 645-654, (2011).
10. He L., Li L., Yu L., Mao E. and Song, J., "A torque-based nonlinear predictive control approach of automotive powertrain by iterative optimization", ***Journal of Automobile Engineering***, 226(8) 1016-1025, (2012).
11. Fang C., Cao Z., Ektesabi M. M., Kapoor A. and Sayem A. H. M., "Model reference control for active drivability improvement", ***International Conference on Modelling, Identification and Control***, Melbourne, 202-206, (2014).
12. Pacejka H., B., "Tyre and Vehicle Dynamics", ***Butterworth-Heinemann***, 9780080970165, Oxford, (2006).
13. Otkur M., Atabay O. and Ereke M., "In Cylinder Pressure Based Brake Torque Model For Diesel Engines", ***International Conference on Automotive & Vehicle Technologies***, *İstanbul,* 182-191, (2013).